An Explainable Classifier Using Diffusion Dynamics for Misinformation Detection on Twitter

Arghya Kundu and Uyen Trang Nguyen
Electrical and Computer Engineering, York University, Toronto, Canada

Keywords: Misinformation, XAI, Social Network, Twitter.

Abstract: Misinformation, often spread via social media, can cause panic and social unrest, making its detection crucial. Automated detection models have emerged, using methods like text mining, usage of social media user properties, and propagation pattern analysis. However, most of these models do not effectively use the diffusion pattern of the information and are essentially black boxes, and thus are often uninterpretable. This paper proposes an ensemble based classifier with high accuracy for misinformation detection using the diffusion pattern of a post in Twitter. Additionally, the particular design of the classifier enables intrinsic explainability. Furthermore, in addition to using different temporal and spatial properties of diffusion cascades this paper introduces features motivated from the science behind the spread of an infectious disease in epidemiology, specially from recent studies conducted for the analysis of the COVID-19 pandemic. Finally, this paper presents the results of the comparison of the classifier with baseline models and quantitative evaluation of the explainability.

1 INTRODUCTION

Misinformation refers to inaccurate or misleading news that is propagated through various digital or analog communication channels. Misinformation is corrosive as it has a propensity to cause panic in the population and social unrest. Studies point out that people refrain from spreading misinformation if they know it to be false (Zubiaga et al., 2016). However, identifying false news is non-trivial and this motivates the effort of misinformation detection. Journalists and fact-checking websites such as PolitiFact.com can be used to track and detect misinformation. However, their underlying methodology is manual, thus being prone to poor coverage and low speed. Therefore, it is necessary to develop automated approaches to facilitate real-time misinformation tracking and debunking.

Most of the previous work related to automated misinformation detection focuses on news content, user metadata, source credibility and propagation cascades. These methods mostly do not consider or tend to oversimplify the structural information associated with misinformation propagation. However, the propagation patterns have been shown to provide useful insights for identifying misinformation.

A landmark study conducted on Twitter found that the diffusion cascades of misinformation is different from that of true information (Vosoughi et al., 2018). Specifically, misinformation propagates significantly farther, faster, deeper, and broader. Moreover, in a separate recent study (Juul and Ugander, 2021) on the same dataset used in (Vosoughi et al., 2018), the authors found that these differences in diffusion patterns on Twitter can be attributed to the "infectiousness" of the posts (tweets). They concluded that misinformation is more "infectious" than true information. While the mentioned studies provide empirical evidence that misinformation can be differentiated based on the propagation cascades and "infectiousness", it remains unclear how it can be properly used to create verifiable automated detection mechanisms.

Additionally, modern AI systems solve complex problems but often produce unexplainable results. For misinformation detection, user trust in the model impacts their view of an article's credibility. Explainable AI (XAI) models produce interpretable results (Mishima and Yamana, 2022). Previous XAI research on misinformation detection has mainly focused on content and social context, often overlooking propagation cascades.

This motivated us to investigate this approach further, focusing solely on diffusion patterns to identify misinformation and provide explanations based on the model's intrinsic properties. In this study, we propose an ensemble misinformation detection model using spatio-temporal and epidemiological features of

Kundu, A. and Nguyen, U.
An Explainable Classifier Using Diffusion Dynamics for Misinformation Detection on Twitter.
DOI: 10.5220/0012990700003838

In *Proceedings of the 16th International Joint Conference on Knowledge Discovery, Knowledge Engineering and Knowledge Management (IC3K 2024) - Volume 1: KDIR*, pages 348-357
ISBN: 978-989-758-716-0; ISSN: 2184-3228

diffusion cascades with intrinsic explanation generations for users. Then, we compare the accuracy of our proposed model against five state-of-the-art misinformation detection models. Finally, we validate the explainability of our model using quantitative metrics.

The contributions of this paper are as follows:

- Firstly, this study only uses propagation patterns of social media posts to develop a misinformation detection model as opposed to most prior work which uses additional characteristics like content-based, source based and style-based methods.
- Secondly, we propose an ensemble system for misinformation detection by applying three classifiers, namely, K-nearest neighbour, decision tree and multilayer perceptron (MLP). Furthermore, the ensemble system is designed in a specific way to always provide intrinsic explainability.
- Thirdly, this paper uses temporal and spatial properties of diffusion cascades, along with features inspired by epidemiology, particularly insights from recent COVID-19 studies.

The paper is structured as follows. Section 2 details the related work. Section 3 discusses the datasets used in the study. Section 4 explains the tweet propagation structures. Section 5 discusses the methodology to build the misinformation detection system. Section 6 focuses on the model's explainability. Section 7 discusses the experimental results. Section 8 details the explainability evaluation. Finally, Section 9 concludes the paper.

2 RELATED WORK

2.1 Automatic Misinformation Detection

Automatic misinformation detection on social media platforms is grounded on the use of traditional classifiers that detect fake news deriving from the pioneering study of information credibility on Twitter (Carlos Castillo and Poblete, 2011). In following works (Xiaomo Liu and Shah, 2015) (Ma et al., 2015), different sets of unique features were used to classify whether a news is credible. Most of these prior works attempted to classify the veracity of spreading news using information beyond the text content, such as post popularity, user credibility features, and more. However, these studies did not take into account the propagation structure of a post. In this paper, we focuses on using the diffusion cascade of the posts (tweets).

Nevertheless, some studies have investigated capturing the temporal traits of a post. One study introduced a time-series-fitting model (Kwon et al., 2013), focusing on the temporal properties of a single feature – tweet volume. Another study (Ma et al., 2015) expanded upon this model by using dynamic time series to capture the variation of a set of social context features. In addition, another study (Friggeri et al., 2014) characterized the structure of misinformation cascades on Facebook by analyzing comments.

However, these studies does not effectively take into account the relevance of the spread of misinformation to that of an infectious disease. In this study we took motivation from the field of epidemiology and account for the spatio-temporal features originating from the study of the spread of infectious diseases, specifically from the recent studies conducted for the analysis of the COVID-19 pandemic.

2.2 Explainability of Models

Approaches to explainable machine learning are generally classified into two categories: intrinsic explainability and post-hoc explainability. Intrinsic interpretability is achieved by constructing self-explanatory models which incorporate interpretability directly to their structures. In contrast, the post-hoc XAI requires creating a second model to provide explanations for an existing model which is considered as a black-box. Studies have shown that intrinsic XAIs provide better explanations than post-hoc XAIs (Du et al., 2018), however they have a trade-off with accuracy. Moreover, existing XAI models for misinformation detection often overlook propagation statistics. This motivated us to design an XAI model that generates explanations solely from diffusion characteristics of the tweet. The proposed model offers both intrinsic explainability and high accuracy.

Nevertheless, evaluating XAI models remains crucial, yet due to the nascent nature of this field, consensus on explanation evaluation is lacking. A recent survey (Mishima and Yamana, 2022) highlighted that many XAI models lack standardized evaluation methods; they often rely on informal assessments or even skip evaluation altogether. In this study, we use three quantitative metrics to evaluate the explainability of our model.

3 DATASET

For evaluation of our model we use the popular publicly available datasets (Ma et al., 2017), Twitter15 and Twitter16, which have been widely adopted as standard data in the field of misinformation detection. Some important characteristics of the dataset are mentioned in Table 1.

Table 1: Basic Statistics of the datasets.

Statistic	Twitter15	Twitter16
# Users	306,402	168,659
# Tweets	331,612	204,820
Max. # retweets	2,990	999
Min. # retweets	97	100
Avg. # retweets	493	479

4 PROPAGATION STRUCTURE REPRESENTATIONS

Propagation networks of information on social media are represented in various ways. For this study we employ the following two representations,

- Hop based structure
- Time based structure

4.1 Hop Based Structure

In this type of structure, the diffusion of a post is represented as a directed acyclic graph, with the root of the tree being the source tweet and the corresponding children being the retweets.

The advantage of using this representation lies in its ability to readily leverage the spatial properties of post diffusion. Additionally, this method of representation effectively captures the user-follower relationship of tweets propagation in Twitter.

4.1.1 Analysis of the Representation

Figure 1a depicts a random news dissemination sample in hop based cascade representation. The source tweet is located at the centre of the biggest cluster and all other nodes represents the successive retweets.

The following observations were made,

- Maximum number of retweets are made directly from the source tweet.
- Most of the graphs have at least one dense cluster which does not include the source tweet i.e the tree has at least one very popular retweet.

4.2 Time Based Structure

In this cascade representation, we calculate the time delay between a retweet and its source tweet. Using this delay, the retweet is positioned on the relevant stack using a sampling time. The sampling time (d) is chosen to be 60 minutes for this study. The advantage of using this representation is the ease of using the temporal properties of the diffusion of a post. This representation effectively captures the life-cycle, popularity of a post and the amount of interactions accounted by the tweet over time.

4.2.1 Analysis of the Representation

Figure 1b depicts a random news dissemination sample in time based propagation representation.
Following are some observations:

- During the first couple of hours the tweet had the farthest spread. That is, the news penetrated with more traction in the social media.
- Most of the plots follow an approximation of power law distribution.

Table 2: Feature Categorization.

Number	Feature	Type
1	Number of Nodes	Spatial Feature
2	Total Diffusion Time	Temporal Feature
3	Total Peaks	Temporal Feature
4	Mean of timestamps delays	Temporal Feature
5	Basic Reproduction Number	Epidemiological Feature
6	Basic Transmission Rate	Epidemiological Feature
7	Super Spreaders	Epidemiological Feature
8	Growth Acceleration	Epidemiological Feature
9	Average Growth Speed	Epidemiological Feature
10	SD of Timestamps Delays	Temporal Feature
11	RMSSD of Timestamps Delays	Temporal Feature
12	Height	Spatial Feature

5 METHODOLOGY

This section details the methodology of our explainable ensemble classifier.

5.1 Feature Selection

The following features are used as referred in Table 2 along with their corresponding feature type.

5.1.1 Number of Nodes

This represents the number of unique users involved in the diffusion of information. Thus, for a news dissemination pattern $N_i = \{R_i, reT_1, reT_j, .., reT_M\}$

$$\text{number of nodes} = \mathbf{card}(N_i) \tag{1}$$

where R_i is the source tweet, reT_j is a retweet and $\mathbf{card}\{S\}$ is the cardinality of the set S.

5.1.2 Total Diffusion Time

This represents the total time taken for the information to propagate in the network, i.e. the life time of

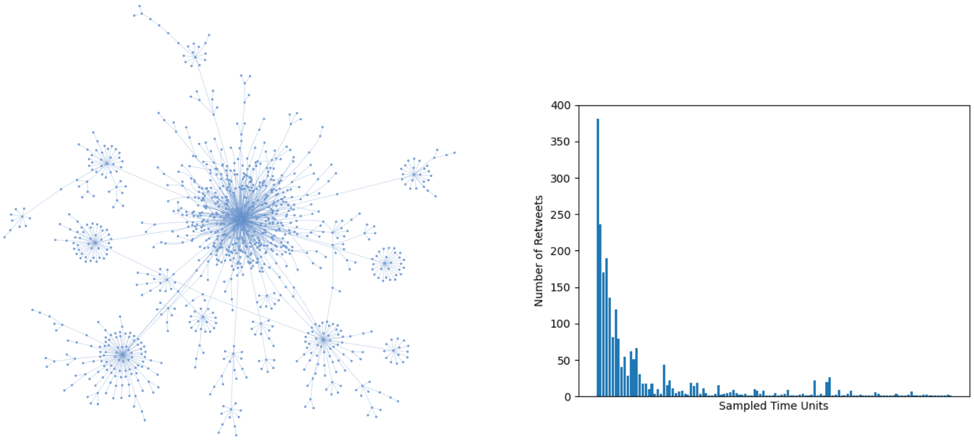

(a) Hop Based Cascade sample

(b) Time Based Cascade sample

Figure 1: Sample Propagation Structure Representations.

the news in Twitter.

$$\text{Total Diffusion Time} = t(reT_M) - t(R_i) \qquad (2)$$

where t(x) is the timestamp of the tweet object x and reT_M is the last retweet

5.1.3 Total Peaks

This feature constitutes the number of nodes having timestamp value greater than the graph mean timestamp. Thus,

$$\text{TP} = \textbf{card}\{v \in V \mid G(v,E)[\text{time}] > mean(G(V,E)[\text{time}])\} \qquad (3)$$

where V are the nodes in the diffusion cascade G(V,E).

5.1.4 Basic Reproduction Number

In epidemiology, the basic reproduction number is the expected number of cases directly generated by one case in a population where all individuals are susceptible to the disease (NG et al., 2006) More precisely, it is the number of secondary infections produced by an infected individual. This number is important in determining how quickly a disease will spread through a population. For this study we define the basic reproduction number (R0) as the number of retweets directly from the source tweet (R_i),

$$\text{R0} = \textbf{card}\{e \in E \mid e \in G(V,e) \wedge G(R_i,e)\} \qquad (4)$$

where R_i is the source tweet and $\textbf{card}\{S\}$ is the cardinality.

5.1.5 Basic Transmission Rate

The Susceptible-Exposed-Infectious (SIR) model is used to render a simple model for the spread of a infectious disease. The basic transmission rate (denoted β) is defined as the number of effective contacts made by an infected person per unit time in a given population. In this study, we interpret basic transmission rate as the number of retweets made during the first day (Td) of the source tweet.

$$\beta = \textbf{card}\{v \in V \mid G(v,E)[\text{time}] \leqslant G(R_i,E)[\text{time}] + Td\} \qquad (5)$$

where R_i is the source tweet and G(V,E) is diffusion cascade.

5.1.6 Super Spreaders

In an investigation conducted (Brainard et al., 2023) to analyze the transmission of coronavirus infections, researchers observed a significant impact on the spread of the virus were attributable to individuals identified as 'super spreaders'. Super spreaders are individuals with greater than average propensity to infect. Within this study, we delineate super spreaders (SS) as the number nodes exhibiting an edge count exceeding the average edge count.

$$\text{SS} = \textbf{card}\{v \in V \mid G(v,E) > mean(E)\} \qquad (6)$$

where G(V,E) is the diffusion cascade and E are the edges.

5.1.7 Growth Acceleration

In epidemiology, Growth Acceleration is defined as the $(cases \setminus day^2)$. Recently, in a study it has been shown that Growth Speed and Growth acceleration are very effective for the analysis of the COVID-19 pandemic (Utsunomiya et al., 2020). In this study, we consider the edges i.e the retweets as the cases and define Growth Acceleration (GA) as follows,

$$GA = \sum_{i=1}^{V} \frac{1}{(G(v,E)[\text{time}] - G(R_i,E)[\text{time}])^2} \qquad (7)$$

where G(V,E) is diffusion cascade and V are the nodes.

5.1.8 Average Growth Speed

Additionally, as mentioned previously Growth speed was also shown to be very effective in the analysis of the COVID-19 pandemic (Utsunomiya et al., 2020). In this study, we define Average Growth Speed (avgGS) as follows,

$$avgGS = \frac{heightG(V,E)}{(\text{avg. timestamps delays})} \tag{8}$$

where (avg. timestamps delays) is the average of all the timestamp delays and *height* of $G(V,E)$ is the length of the longest path from the root to the farthest node in the diffusion tree.

5.1.9 Standard Deviation of Timestamps Delays

Using this feature we try to take into account the measure of the spread of values from the mean.

$$\sigma = \sqrt{\frac{1}{V-1}\sum_{i=1}^{V}(t_i - \bar{t})^2} \tag{9}$$

where t are the individual timestamp delays of each retweet from the source tweet.

5.1.10 RMSSD of Timestamps Delays

We also consider the root mean square of successive differences between retweet timestamps (RMSSD). In medical science, RMSSD is considered the primary time domain measure used to estimate the vagally mediated changes (Minarini, 2020). RMSSD reflects the peak-to-peak variance in a time series data. As mentioned in subsection 4.2.1, during the initial stages of propagation, claims exhibit the widest spread, with minimal successive differences between retweets. Consequently, we integrated RMSSD as a feature in our model to capture early-hour changes in news dissemination flow.

$$\text{RMSSD} = \sqrt{\text{mean}\{\text{diff}\{t1, t2, .., tN\}^2\}} \tag{10}$$

where t are the individual timestamp delays of each retweet from the source tweet.

5.1.11 Height

Represents the length of the path from source tweet to its farthest retweet node.

$$\text{Height} = \sum_{R_i}^{reT_n} 1 \tag{11}$$

where R_i is the source tweet and reT_n is the farthest retweet.

5.2 Data Preparation

Firstly, The datasets contained four annotations namely true rumours, non-rumours, false rumours and unverified rumours. As our study focuses on binary classification, we re-annotated to two class labels namely, true and fake news and disregarded the unverified rumours. Secondly, we normalized the features by scaling and translating. We used the Min Max Normalization method. Finally, For a fair comparison,we randomly split the datasets into 80% for training and 20% for testing.

5.3 Classification Model

For this study we used a voting classifier. A voting classifier is a ensemble machine learning classifier that trains various base models and predicts on the basis of aggregating the findings of each base estimator. Voting classifiers has been shown to reduce the aggregate errors of a variety of the base models and increase final accuracy. The aggregating criteria used in this study is hard voting which is the combined decision of the class label that has been predicted most frequently by the classification models. The base models used are as follows, refer Figure 2 :

- KNN Classifier
- Decision Tree Classifier
- Multi-layer Perceptron classifier

Thus, the predicted class label $\hat{y}$ of our proposed classifier is as follows,

$$\hat{y} = \text{mode}\{C_1(x), C_2(x), C_3(x)\} \tag{12}$$

where $C_i(x)$ is the predicted class label of classifier i.

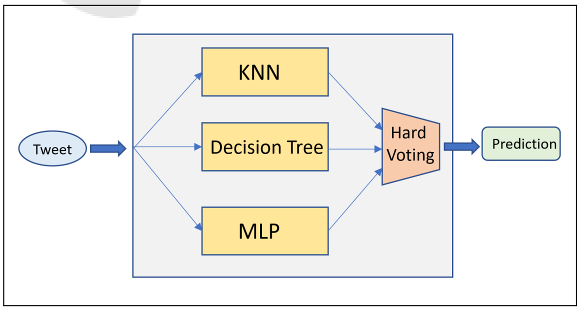

Figure 2: Voting Classifier Flowchart.

6 EXPLANABILITY OF MODEL

Research shows that intrinsic explainable AI (XAI) provide better explanations than post-hoc XAIs (Du et al., 2018), though sometimes with reduced accuracy. Our method balances intrinsic model explanations via KNN and decision tree (DT) classifiers while maintaining high accuracy.

The following two methods were used to accomplish this,

- Firstly, the unique design of the ensemble classifier asserts that at least one intrinsic explainable classifier is part of the final aggregated vote. That is, in the best case scenario both the intrinsic explainable classifiers (KNN or DT) have the same predicted label. Whereas, in the average/worst case scenario along with MLP classifier either KNN or DT classifier has the same predicted label which can be used to provide intrinsic explainability.
- Secondly, we added MLP to balance the accuracy-explainability trade-off in intrinsic XAIs. Although, MLP is not an intrinsic explainable algorithm on its own, the combination the three classifiers provides intrinsic explainability along with high accuracy.

6.1 KNN Classifier

In system interpretability, KNN relies on similarity and distance, making it inherently interpretable as the nearest neighbors provide explanations.

For providing human readable explanations for a given prediction, we employed the following steps:

1. Collect nearest K neighbours of considered point (*P*).
2. Filter out same-class neighbors of *P*, which are inherently higher in number.
3. Project (P_{new}) using arithmetic mean of filtered points.
4. Get the four highest correlated features between P_{new} and *P* using Manhattan distance.
5. Display the number of nearby same class label neighbours and the highest correlated features.

6.2 Decision Tree Classifier

A decision tree provides a hierarchy of very specific questions and predicts outcomes based on decision rules (if-then-else rules). The answer to one question guides the prediction process down various branches of the tree. At the bottom of the tree is the prediction. Hence, for interpretations, we review decisions by traversing top-to-bottom tree paths and noting question responses for explanations. To this direction we used the following steps,

1. Fetch the decision rules from the classifier.
2. Use the rules to showcase the answers the specific rule addresses.
3. Every rule corresponds to one feature, delivering a local explanation for that feature's value.
4. For a given point (*P*), traversing the decision tree from top to bottom reveals explanations for the predicted class label. Inherently the number of the explanations is the depth of the decision tree.

7 EVALUATION OF CLASSIFICATION MODEL

In this section we discuss the results of the individual and ensemble classifiers. We used Twitter16 dataset for selecting the parameters and Twitter15 for testing.

7.1 Individual Classifiers

7.1.1 KNN Classifier

The number of neighbors used in this model is ten. Table 3 shows the results from the k-nearest neighbors classifier with varying hyper-parameters. From the table, we can see that the model using Manhattan as the distance metric performs the best, achieving the highest accuracy and precision, along with a good overall recall. This is rational as studies have shown that Manhattan distance (L1 norm) ususally performs better than common distance measures in the case of high dimensional data.

Table 3: Results of the KNN classifier on Twitter16.

Distance metric	Accuracy	Precision	Recall
Cosine	0.8123	0.8436	0.8787
Manhattan	**0.8129**	**0.8591**	0.8865
Correlation	0.8045	0.7899	**0.8934**
Euclidean	0.8104	0.8087	0.8799
BrayCurtis	0.7903	0.7832	0.8811

7.1.2 Decision Tree Classifier

The maximum depth of the tree is chosen to be three, in order to reduce computational complexity. Table 4 depicts the results with varying hyper-parameters. It can be observed that the results are better with the entropy splitting criterion. However, the accuracy is almost the same for both the splitting methods. This is reasonable as the internal working of both the splitting methods are very similar. Nevertheless, for the ensemble model we choose the entropy criterion.

Table 4: Results of the Decision Tree classifier on Twitter16.

Splitting criterion	Accuracy	Precision	Recall
Gini	0.8117	0.8548	0.8676
Entropy	**0.8123**	**0.8679**	**0.8815**

7.1.3 Multi-Layer Perceptron Classifier

The MLP classifier has been configured with two hidden layers containing (5,2) units respectively. Limited-memory BFGS (lbfgs) algorithm has been used for weight optimization as it converges faster and performs better for small datasets. Table 5 depicts the results. It can be observed from the results that the accuracy and recall is highest with the Sigmoid activation function. As the number of hidden layers is very low in this model the vanishing gradient problem does not play a significant role and hence the accuracy using sigmoid function is higher compared to other activation functions.

Table 5: Results of the MLP classifier on Twitter16.

Activation function	Accuracy	Precision	Recall
Tanh	0.7945	0.7712	**0.9117**
Sigmoid	**0.8231**	**0.8574**	0.8905
ReLU	0.8117	0.8419	0.8620

7.2 Ensemble Classifier

The results for the individual classifiers are shown in Table 6 with the optimum parameter configurations. Firstly, It can be observed that MLP classifier has the highest accuracy of 82.31%, however the precision is low with 0.8574.

Table 6: Results of the individual classifiers on Twitter16.

Type	Accuracy	Precision	Recall
KNN classifier	0.8129	0.8591	0.8865
MLP classifier	**0.8231**	0.8574	**0.8905**
Decision tree classifier	0.8123	**0.8679**	0.8815

Secondly, the KNN classifier also has a high accuracy of 81.29% with the low recall and precision. Finally, the precision is highest in the case of the decision tree classifier with 0.8679, with an accuracy almost similar to that of the KNN classifier. Thus, it can be reasoned that a combination of these three classifiers might produce better results. This motivated us to implement an ensemble voting classifier for this study.

Table 7 depicts the results for the Voting Classifier.

Table 7: Results of the Voting Classifier on Twitter16.

Type	Accuracy	Precision	Recall
Voting Classifier	**0.8522**	**0.8843**	**0.8917**

It can be inferred from Table 7 that the accuracy has increased to 85.22 % with the use of the voting classifier. Ensemble methods like the voting classifier are ideal for reducing the variance in models, thereby increasing the accuracy of predictions. The variance is eliminated when multiple classifiers are combined to form a single prediction. Additionally, it can be observed that the precision and recall of the voting classifier are also high with 0.8843 and 0.8917 respectively. From our experiments, it can be reasoned that the voting ensemble outperforms all the individual models.

7.3 Baseline Model Comparison

We compared our proposed model with the following five state-of-the-art misinformation detection models,

1. CSI (Ruchansky et al., 2017): A misinformation detection model that captures temporal patterns using an LSTM to analyze user activity and calculates user scores.
2. tCNN (Yang et al., 2023): a modified convolution neural network that learns the local variations of user profile sequence, combining with the source tweet features.
3. CRNN (Liu and Wu, 2018): a state-of-the-art joint CNN and RNN model that learns local and global variations of retweet user profiles, together with the resource tweet.
4. dEFEND (Shu et al., 2019): a state-of-the-art co-attention-based misinformation detection model that learns the correlation between the source article's sentences and user profiles.
5. GCAN (Lu and Li, 2020): a state-of-the-art graph-aware co-Attention network based misinformation classifier that uses user profiles metadata, news content and propagation pattern.

Table 8 compares our approach to the industry standards. It can be inferred that our proposed model outperforms most of the state-of-the-art approaches on both datasets in terms of accuracy while attaining highest precision and recall. In particular, our model achieves an accuracy of 84.47% and 85.22% on the datasets respectively. Although GCAN achieved the highest accuracy, the precision and recall are low due to the class imbalance in the datasets, where GCAN favors the majority class, leading to higher accuracy but poorer minority class detection. Whereas, our model received at par accuracy with GCAN with higher precision and recall. Furthermore, GCAN in addition to propagation pattern uses the user profile metadata and tweet content, which might not always be available in real-world scenarios. Whereas, our model solely uses the diffusion pattern to create a classifier.

Table 8: Experimental results on Twitter15 (T15) and Twitter16 (T16) datasets.

Method	Recall		Precision		Accuracy	
	T15	T16	T15	T16	T15	T16
tCNN	0.5206	0.6262	0.5199	0.6248	0.5881	0.7374
CRNN	0.5305	0.6433	0.5296	0.6419	0.5919	0.7576
CSI	0.6867	0.6309	0.6991	0.6321	0.6987	0.6612
dEFEND	0.6611	0.6384	0.6584	0.6365	0.7383	0.7016
GCAN	0.8295	0.7632	0.8257	0.7594	**0.8767**	**0.9084**
Our model	**0.8512**	**0.8917**	**0.8568**	**0.8843**	0.8447	0.8522

7.4 Ablation Study

To study the contribution of each feature type towards the ensemble classifier, we carry out ablation experiments. The results are shown in Table 9. The ablation experiments include the following three variants:

- w/o Spatial: Removing the spatial features of the ensemble classifier.
- w/o Temporal: Removing the temporal components of the ensemble classifier.
- w/o Epidemiological: Removing the epidemiological features of the ensemble classifier.

Table 9: Results of the Ablation experiments using Twitter16.

Type	Accuracy	Precision	Recall
w/o Spatial	0.8213	0.8229	0.8078
w/o Temporal	0.8256	0.8594	0.8810
w/o Epidemiological	0.7714	0.7803	0.8276
Voting classifier	**0.8522**	**0.8843**	**0.8917**

From Table 9, we can observe that all ablation variants drop some accuracy compared with the primary model. Specifically, when removing the spatial features, the accuracy drops by 3.1%, the precision and recall also dropped. The replacement of the temporal features caused the accuracy to decrease by 2.7% with lower precision and recall. However, the accuracy drop was most significant when the epidemiological features were removed, accounting to 8.1% along with lowest precision and recall. This corroborates that epidemiological features inspired from the study on COVID-19, play an essential role for misinformation detection using propagation cascades. In conclusion, overall the primary model, with the three component types involved, provides a better choice compared to the ablation variants.

8 EVALUATION OF EXPLAINABILITY OF THE MODEL

Evaluation of an XAI model essential, as it provides a way to understand its practical implication.

8.1 Sample Explanation

Figure 3 displays the explanations generated by our model on a random data point (*P*), where KNN classifier and DT classifier had the same predicted class label. We can observe that, three explanations were generated for the DT classifier, which is logical as the depth of the tree was three. Furthermore for point *P*, the KNN classifier interpretations were made from the seven nearby fake tweets out of the ten neighbours. An interesting observation can also be made that explanations for both the classifiers almost correspond for the same statistical properties of the propagation cascade.

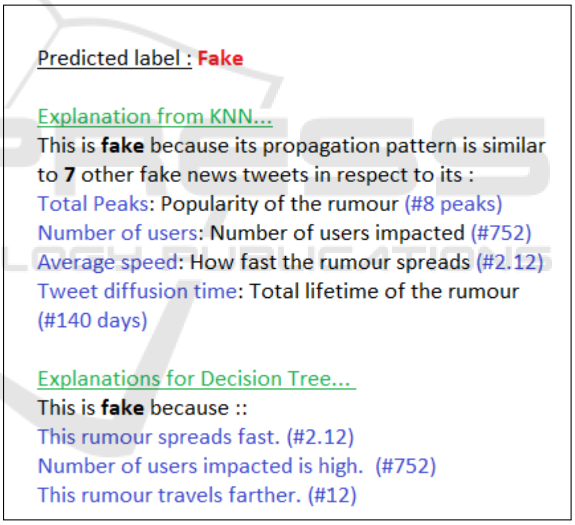

Predicted label : **Fake**

Explanation from KNN...

This is **fake** because its propagation pattern is similar to **7** other fake news tweets in respect to its :

Total Peaks: Popularity of the rumour (#8 peaks)

Number of users: Number of users impacted (#752)

Average speed: How fast the rumour spreads (#2.12)

Tweet diffusion time: Total lifetime of the rumour (#140 days)

Explanations for Decision Tree...

This is **fake** because ::

This rumour spreads fast. (#2.12)

Number of users impacted is high. (#752)

This rumour travels farther. (#12)

Figure 3: Explanation generated for a random sample (*P*).

8.1.1 Metrics Used

We evaluated the model's interpretability using the three metrics mentioned below. These are extensions of three metrics used in (ElShawi et al., 2021) for evaluating interpretability frameworks like LIME, SHAP, LORE and more.

- *Stability*: Similar instances should have similar explanations.
- *Separability*: Different instances should yield different explanations.
- *Identity*: Identical instances must produce identical explanations.

For measuring the metrics we randomly select 100 data points and create the testing dataset using their class labels and generated explanations. The stability metric is measured by applying K-means clustering with two clusters to group explanations in the testing dataset. For simplicity, we use the three explanations generated by the decision tree (DT), converting each explanation string into a unique numerical value to form an integer array. The assigned cluster labels are then compared with the predicted class labels to evaluate whether instances of the same class have similar explanations. To measure the separability metric, two subsets S1 and S2 of the testing dataset are selected corresponding to different class labels. Then, for each instance in S1, its explanation is compared with all other explanations of instances in S2. If the explanation have no duplicates, it satisfies the separability metric. Finally, the identity of the explanations offered by the various deterministic techniques may be easily measured theoretically. The explanations generated by the decision tree is rule based thus conforming to complete identity conservation. Additionally, due to the nature of KNN alrogithm identical instances will have identical explanations.

8.1.2 Results

The experimental findings can be seen in Table 10. The figures in this table show the percentage of instances that meet the specified metrics. From the table we can infer that identity metric is 100%, as identical instances will have a similar explanations. The stability is very high, thus conforming that instances with same class labels have comparable interpretations. Finally, the separability is also very high, thus acknowledging that dissimilar instances have dissimilar explanations.

9 CONCLUSION

This paper demonstrates the effectiveness of an ensemble-based classifier using a tweet's diffusion pattern for accurate misinformation detection. We improve the classification by using features inspired by epidemiology and recent COVID-19 research, while providing understandable predictions. The intrinsic explanations help users to understand the predicted class label without compromising accuracy.

Future work will focus on the following areas:

- Incorporating statistical and qualitative measures to evaluate the results and generated explanations.
- Expanding the model's applicability to other social networks such as Instagram and Facebook.
- Investigate and document how hyperparameters, such as the value of k in k-NN, sampling rate, affect model performance.
- Conduct deeper analysis on the consistency and comparability of explanations generated by different models (e.g., k-NN vs. DT).

Table 10: Metrics for the evaluation of explanations.

Metric	Score
Stability	89%
Separability	97%
Identity	100%

REFERENCES

Brainard, J., Jones, N. R., Harrison, F. C., Hammer, C. C., and Lake, I. R. (2023). Super-spreaders of novel coronaviruses that cause sars, mers and covid-19: a systematic review. *Annals of Epidemiology*, 82:66–76.e6.

Carlos Castillo, M. M. and Poblete, B. (2011). Information credibility on twitter. page 675–684.

Du, M., Liu, N., and Hu, X. (2018). Techniques for interpretable machine learning.

ElShawi, R., Sherif, Y., Al-Mallah, M., and Sakr, S. (2021). Interpretability in healthcare: A comparative study of local machine learning interpretability techniques. *Computational Intelligence*, 37(4):1633–1650.

Friggeri, A., Adamic, L., Eckles, D., and Cheng, J. (2014). Rumor cascades. *Proceedings of the 8th International Conference on Weblogs and Social Media, ICWSM 2014*, pages 101–110.

Juul, J. L. and Ugander, J. (2021). Comparing information diffusion mechanisms by matching on cascade size. *Proceedings of the National Academy of Sciences*, 118(46).

Kwon, S., Cha, M., Jung, K., Chen, W., and Wang, Y. (2013). Prominent features of rumor propagation in online social media. In *2013 IEEE 13th International Conference on Data Mining*, pages 1103–1108.

Liu, Y. and Wu, Y.-F. (2018). Early detection of fake news on social media through propagation path classification with recurrent and convolutional networks. *Proceedings of the AAAI Conference on Artificial Intelligence*, 32(1).

Lu, Y.-J. and Li, C.-T. (2020). GCAN: Graph-aware co-attention networks for explainable fake news detection on social media. In *Proceedings of the 58th Annual Meeting of the Association for Computational Linguistics*.

Ma, J., Gao, W., Wei, Z., Lu, Y., and Wong, K.-F. (2015). Detect rumors using time series of social context information on microblogging websites.

Ma, J., Gao, W., and Wong, K.-F. (2017). Detect rumors in microblog posts using propagation structure via kernel learning. In *Proceedings of the 55th Annual Meeting of the Association for Computational Linguistics (Volume 1: Long Papers)*.

Minarini, G. (2020). Root mean square of the successive differences as marker of the parasympathetic system and difference in the outcome after ans stimulation. In Aslanidis, T., editor, *Autonomic Nervous System Monitoring*, chapter 2. IntechOpen, Rijeka.

Mishima, K. and Yamana, H. (2022). A survey on explainable fake news detection. *IEICE Trans. Inf. Syst.*, E105.D(7):1249–1257.

NG, B., K, G., B, B., and Caley P, Philp D, M. J. (2006). Using mathematical models to assess responses to an outbreak of an emerged viral respiratory disease. *National Centre for Epidemiology and Population Health*.

Ruchansky, N., Seo, S., and Liu, Y. (2017). Csi: A hybrid deep model for fake news detection. pages 797–806.

Shu, K., Cui, L., Wang, S., Lee, D., and Liu, H. (2019). Defend: Explainable fake news detection. In *Proceedings of the 25th ACM SIGKDD International Conference on Knowledge Discovery & Data Mining*, KDD '19, page 395–405, New York, NY, USA. Association for Computing Machinery.

Utsunomiya, Y. T., Utsunomiya, A. T. H., Torrecilha, R. B. P., de Cássia Paula, S., Milanesi, M., and Garcia, J. F. (2020). Growth rate and acceleration analysis of the covid-19 pandemic reveals the effect of public health measures in real time. *medRxiv*.

Vosoughi, S., Roy, D., and Aral, S. (2018). The spread of true and false news online. *Science*, 359:1146–1151.

Xiaomo Liu, Armineh Nourbakhsh, Q. L. R. F. and Shah, S. (2015). Real-time rumor debunking on twitter. page 1867–1870.

Yang, Y., Zheng, L., Zhang, J., Cui, Q., Li, Z., and Yu, P. S. (2023). Ti-cnn: Convolutional neural networks for fake news detection.

Zubiaga, A., Liakata, M., Procter, R., Wong Sak Hoi, G., and Tolmie, P. (2016). Analysing how people orient to and spread rumours in social media by looking at conversational threads. *PLOS ONE*, 11(3):1–29.